

Active Anti-Islanding Protection For Grid Connected Solar Photovoltaic Power Plant

Rose Therese K Jose*, Nisha R**, Ramesh P***, Jiju K***

*PG Scholar, **Assistant Professor Department of Electrical and Electronics Toc H Institute of Science and Technology Ernakulam, India.

***Senior Engineer Power Electronics Group Centre for Development of Advanced Computing – CDAC Trivandrum, India.

Abstract

Islanding detection and anti-islanding protection is an important concern in grid connected solar photovoltaic (PV) system due to utility service personnel and equipment safety. The aim of this paper is to analyse, design, implement and evaluate an active anti-islanding method in solar photovoltaic power plants. Active methods introduce a deliberate disturbance into the system, and monitor the disturbance effect for islanding detection. An active islanding detection method using voltage harmonic injection into the reference modulating signal is proposed in this study. The proposed method is based on injecting small voltage harmonics into the PWM modulator in order to detect the islanding event. The performance of the proposed method has been studied using simulations in POWERSIM platform and the results are presented to highlight the effectiveness of the method.

Keywords: Anti-islanding, Active Anti-islanding, Islanding, PV System, Passive Anti-islanding, Voltage Harmonic Injection.

I. INTRODUCTION

Distributed generation for renewable energy sources is penetrating the electric power system due to the rising cost of traditional energy sources and the environmental friendly features of renewable energy. The types of renewable energy include solar, wind, hydrogen, biomass, geothermal, hydropower, and biodiesel. The photovoltaic-based generation has gained importance in DG systems due to its clean, affordable, and available technology. However, there are also challenges associated with the DG, among which islanding detection is an important and difficult one. An islanding is a condition in which a portion of an Area Electric Power System (EPS) is energized solely by one or more Local EPSs through the associated point of common coupling (PCC) while that portion of the Area EPS is electrically separated from the rest of the Area EPS [1].

An island may occur due to many reasons such as, a disconnection for servicing, human error, an act of nature, or one of the circuit breakers in the power system trips as with distributed generation (DG). Under islanding condition, the distributed resource (DR) is required to disconnect within 2 seconds according to IEEE 1547 [1].

There are two types of islanding: intentional islanding and inadvertent islanding [1-2]. Typically, intentional islanding is harmless to the power system because the problem can be solved during or after the grid disconnection [1]. However, unintentional

islanding can create a severe impact to the power system stability due to the loss of grid synchronization. Consequently, this causes the DG to be out of the voltage and frequency references. This may damage the electrical devices and systems equipment in the islanded section. Another issue persists in the islanding mode whereby the technical workers may be placed under safety hazards as they may not be aware that the section is continuously powered by the DG. For this reason, anti-islanding control is essential in order to detect the islanding operation immediately.

There are mainly three types of islanding detection methods which includes communication-based, passive [3], and active methods [4]. The communication-based methods do no harm the power quality of the power system with the negligible non-detection zone (NDZ), the cost is much higher than the other two types of methods and the operations are more complex as well [4]. A passive method monitors voltage, frequency and phase and then compares those with threshold limits. It is usually difficult with passive techniques to set thresholds to prevent both islanding and nuisance trips at the same time. Although the methods are economically attractive due to their simplicity, the existence of large non detection zone (NDZ) is a major drawback [5]. The active methods rely on injecting intentional disturbances or harmonics into some DG parameters to identify whether islanding has occurred [6]–[7].

The active frequency drift [8], slip-mode frequency shift [9], and Sandia frequency shift [10] methods are three classical active methods by creating a continuous trend to change the frequency during islanding. Though active methods suffer smaller NDZs, the presence of disturbances during normal operation will sacrifice power quality and reliability of the power system. But the power quality issue can be reduced by injecting the disturbance signal in a cyclic manner.

Voltage source inverters (VSI) are used for energy conversion from a DC source to an AC output, both in a standalone mode or when connected to the utility grid. A filter is required between a VSI and the grid, imposing a current-like performance for feedback control and reducing harmonics of the output current. Here LCL filter is used in place of conventional L filter. The LCL filter reduces the switching frequency ripple and helps in coupling with a current-like performance to the utility grid. It achieves a higher attenuation along with cost savings, given the overall weight and size reduction of the components [11-14].

II. SYSTEM SET-UP FOR ISLANDING DETECTION

In this study, we consider a three-phase grid connected solar photovoltaic power plant which consists of a dc source (solar photovoltaic array), an inverter, a LCL filter, a delta- star transformer, a controller and utility grid in order to implement the islanding event. The Fig. 2.1 below shows the single line diagram of grid connected solar photovoltaic system, which is the islanding test setup used in the study.

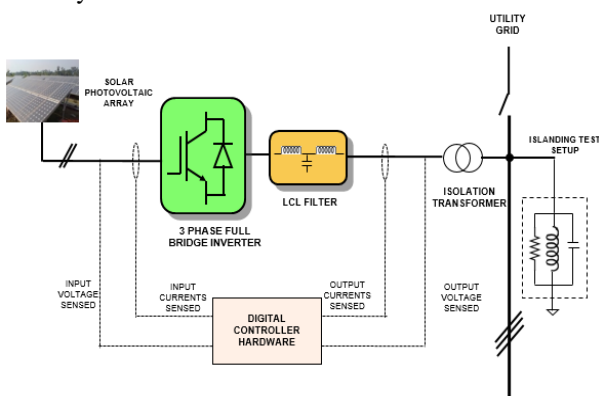


Fig. 2.1: Single line diagram of Grid connected Solar Photovoltaic System

A 10 kWp solar photovoltaic prototype is considered in the study. A grid connected inverter is a power inverter that converts direct current (DC) electricity into alternating current (AC) with an ability to synchronize to interface with a utility line. It synchronizes its frequency with that of grid (50 Hz). They are also designed to quickly disconnect from the

grid if the utility grid goes down. In place of L filter here a LCL filter is used. LCL filter provides inductive output at the grid interconnection point to prevent inrush current compared to LC filter and has better attenuation. The controller plays a key role in operating, managing, and protecting the DG system. The controller used was a current controlled proportional integral controller.

III. ISLANDING STANDARDS FOR A GRID CONNECTED PHOTOVOLTAIC SYSTEM

As per the current standard IEEE 1547.4 [15], "Guide for Design, Operation and Integration of Distributed Resource Island Systems with Electric Power Systems", published in 2011, there are some islanding standards for grid connected solar photovoltaic (SPV) power plant. Table 3.1 and 3.2 indicates the clearing time information for DG disconnection during under and over voltage and frequency events.

Table 3.1: IEEE 1547.4 Voltage Standard Settings

Voltage (at PCC)	Maximum trip time (s)
$V < 50\%$	0.16
$50\% < V < 88\%$	2.00
$88\% \leq V \leq 110\%$	Continuous operation
$110\% \leq V \leq 120\%$	1.00
$120\% \leq V$	0.16

Table 3.2: IEEE 1547.4 Frequency Standard Settings

Frequency Range (50 Hz = Normal Operation)	Clearing time(s)
$< 49\text{Hz}$	0.16
$49\text{ Hz} \leq \text{Freq} \leq 51\text{ Hz}$	Continuous operation
$> 51\text{ Hz}$	0.16

IV. ACTIVE ANTI-ISLANDING METHOD

Passive methods are the one which are commonly used for the islanding detection applications since they are simple and easy to implement. But they have large non- detection zones (NDZ) and is not possible for smart grid applications. So active anti-islanding method are preferred. It has very small NDZs. The worst conditions of anti-islanding are given below.

1. The power generated by DG should match the R-L-C load power $\Delta P=0$ and $\Delta Q=0$.
 2. Resonant frequency of R-L-C load is same as grid frequency ($f=50\text{Hz}$).
 3. The Q factor of R-L-C load is set to be 2.5.
- During worst conditions, the islanding detection is very difficult mainly in case of passive anti-

islanding scheme. In this situation active islanding methods are applicable. The main idea of the active anti-islanding method is to inject small disturbances like harmonics into the system parameters and read back the same and observe the changes in the parameters in order to detect the islanding condition. The Fig. 4.1 shows the working of the proposed active anti-islanding algorithm.

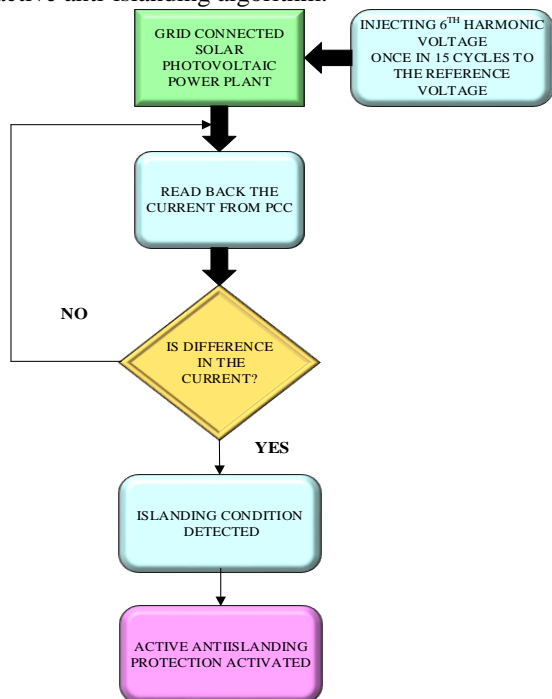


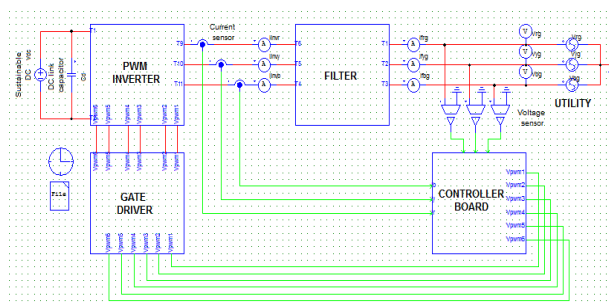
Fig. 4.1: Proposed Active Anti-islanding Protection Algorithm

The active methods have higher accuracy and more reliability than passive anti-islanding methods. However, major drawbacks of the active anti-islanding method include the tendency to disrupt the power quality of the system, high cost, and sensitivity to changes in the power factor at PCC. But in actual case, it is introduced only once in 15 cycles there will not be any serious effect on the power quality.

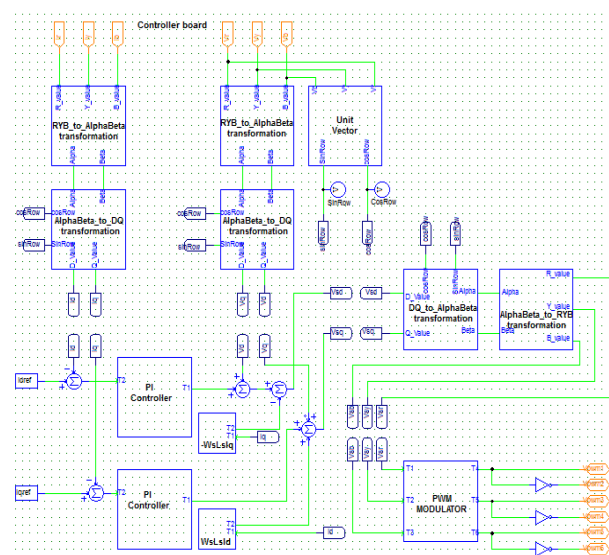
V. MATHEMATICAL MODELLING

5.1 Design of Grid connected Solar Photovoltaic Power System with its Controller

In the simulation model of the grid connected solar photovoltaic power plant, the sustainable dc source along with dc link capacitor represents the solar photovoltaic model and three-phase ac source represents the utility grid. The other blocks used in the simulation include PWM inverter, LCL filter and a controller board as shown in Fig. 5.1(a) and (b). The system was modelled in unity power factor. As the switching frequency of inverter is in medium frequency range (10 kHz), IGBT switches are preferred for the simulation.



(a)



(b)

Fig. 5.1: (a) Simulation diagram of Grid connected Solar Photovoltaic Power Plant without Islanding, (b) its Controller Board

The controller used here is a current controlled PI controller. The controller is used for generating switching signals for the PWM modulator. The mathematical equations given below were used for the modelling of the controller board.

$$V_{sd} = i_{sd} R_s + L \frac{di_{sd}}{dt} - \omega_s Li_{sq} + V_g \quad (5.1)$$

$$V_{sq} = i_{sq} R_s + L \frac{di_{sq}}{dt} + \omega_s Li_{sd} \quad (5.2)$$

The above equations can be rearranged as follows,

$$U_d = i_{sd} R_s + L \frac{di_{sd}}{dt} \quad (5.3)$$

$$U_q = i_{sq} R_s + L \frac{di_{sq}}{dt} \quad (5.4)$$

Where,

$$U_d = V_{sd} + \omega_s Li_{sq} - V_g \quad (5.5)$$

$$U_q = V_{sq} - \omega_s Li_{sd} \quad (5.6)$$

The system parameters used in simulation are given in the Table 5.1.

Table 5.1: System Parameters

Sl. No.	Parameters	Value
1	Sustainable DC Source, V_{dc}	750 V
2	DC Link Capacitor, C_d	355.46 μ F
3	Filter Inductance, $L_1=L_2$	4.765mH
4	Filter Capacitance, C	3.472 μ F
5	Inverter Switching Frequency	10 kHz
6	Grid Voltage, $V_{l-l\text{ rms}}$	415 V

The Fig. 5.2 shows the simulation model of grid connected solar photovoltaic power plant with islanding during no load condition. A three-phase bidirectional switch was used for implementing the islanding event.

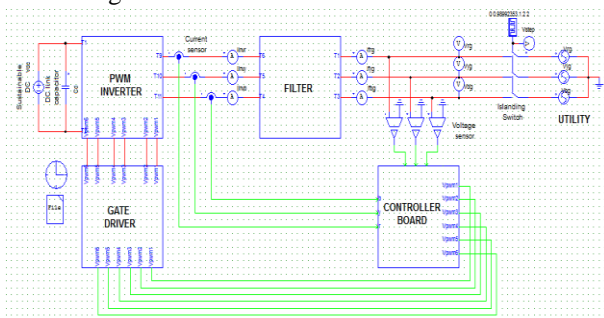


Fig. 5.2: Simulation diagram of Grid connected Solar Photovoltaic Power Plant with Islanding

The Fig. 5.3 shows the simulation model of grid connected solar photovoltaic power plant with islanding with a three-phase parallel R-L-C load.

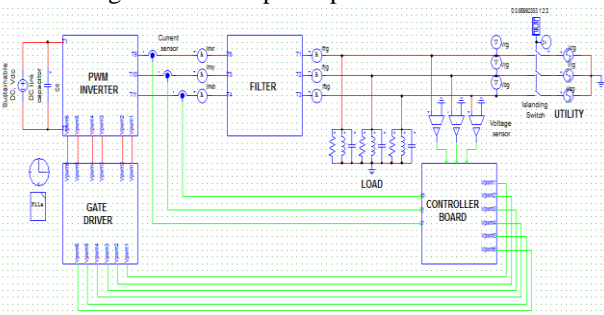


Fig. 5.3: Simulation diagram of Grid connected Solar Photovoltaic Power Plant with parallel R-L-C Load

5.2 Generation of Unit Vector

The unit vector generation is an important part in the simulation. In order to do the transformations, we require cos and sin unit vectors usually represented as $\cos \theta$ and $\sin \theta$ respectively. Since they help us to get the projection of vectors along a particular direction they are referred to as Unit vectors. The Fig. 5.4 shows the phasor diagram showing the unit vectors.

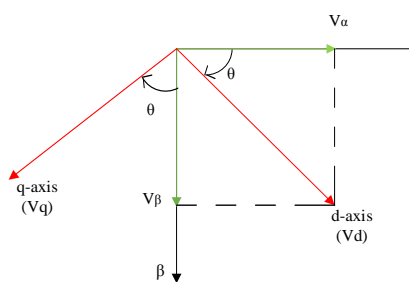


Fig. 5.4: Unit Vector

From the Fig. 6, we have,

$$\cos \theta = \frac{|V_{\alpha}|}{|V|} = \frac{\frac{3}{2}V_m \sin(\omega t)}{\frac{3}{2}V_m} = \sin(\omega t) \quad (5.7)$$

$$\sin \theta = \frac{|V_{\beta}|}{|V|} = \frac{-\frac{3}{2}V_m \cos(\omega t)}{\frac{3}{2}V_m} = -\cos(\omega t) \quad (5.8)$$

From the above derivation, it is evident that the unit vectors can be generated by transforming the grid voltage to α - β plane and then dividing the α -component and β -component by the magnitude of the space vector $\sqrt{|V_{\alpha}|^2 + |V_{\beta}|^2}$. The unit vector implemented using the PSIM software was shown in Fig. 5.5 below.

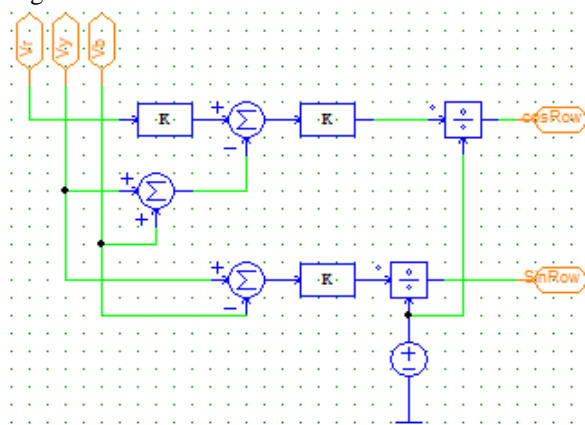


Fig. 5.5: Simulation diagram showing Unit Vector Generation

5.3 Calculation of Load values

Islanding may happen in any section of a grid i.e. in transmission lines, substations, distribution lines, etc. The Tables 5.2, 5.3, and 5.4 below shows the Load values which represents various power levels. In order to find R-L load and R-L-C load the term Quality Factor (Q_f). Quality factor for a parallel R-L-C load is given by,

$$Q_f = \frac{R}{X_L} = \frac{R}{L\omega} \quad (5.9)$$

$$Q_f = \frac{R}{X_C} = RC\omega \quad (5.10)$$

Table 5.2: R Load Values in Ohms and their Power Consumptions

Power (kW)	Resistance (Ω)
1	5.9658
10	59.658
15	89.484

Table 5.3: R-L Load Values for Some Selected Q Factors

Q _f	Resistance 5.9658 Ω	Resistance 59.658 Ω	Resistance 89.484 Ω
	Inductance (mH)	Inductance (mH)	Inductance (mH)
1	18.989	189.897	284.836
2	9.495	94.949	142.418
2.5	7.596	75.959	113.935
4	4.747	47.474	71.209

Table 5.4: R-L-C Load Values for Some Selected Q Factors

Q _f	Resistance 5.9658 Ω	Resistance 59.658 Ω	Resistance 89.484 Ω
	Capacitance (μF)	Capacitance (μF)	Capacitance (μF)
1	533.63	53.36	35.57
2	1067.26	106.71	71.14
2.5	1334.07	133.39	88.929
4	2134.52	213.42	142.29

5.4 Concept of Non Detection Zone

The importance of Active anti-islanding comes where Passive anti-islanding fails. Passive islanding detection methods are based on the power mismatch $\Delta P + j\Delta Q$ and the thresholds of OVP/UV (V_{max}, V_{min}) and OFP/UF (f_{max}, f_{min}). Once the change of the voltage frequency of PCC exceeds outside of the prescribed limits, the OFP/UF, OVP/UV are triggered to prevent islanding. If the change doesn't exceeds outside of prescribed limits, the islanding will occur and the corresponding area of ΔP and ΔQ is defined as the Non- Detection Zone (NDZ). The relationship between the power mismatch and the thresholds of OVP/UV, OFP/UF (V_{max}, V_{min}, f_{max}, and f_{min}) was given in the equations below and it was shown in Fig.5.6.

The NDZ for active power was given by,

$$\left(\frac{V}{V_{max}}\right)^2 - 1 \leq \frac{\Delta P}{P} \leq \left(\frac{V}{V_{min}}\right)^2 - 1 \tag{5.11}$$

The NDZ for reactive power was given by,

$$Q_f \left(1 - \left(\frac{f}{f_{max}}\right)^2\right) \leq \frac{\Delta Q}{P} \leq Q_f \left(1 - \left(\frac{f}{f_{min}}\right)^2\right) \tag{5.12}$$

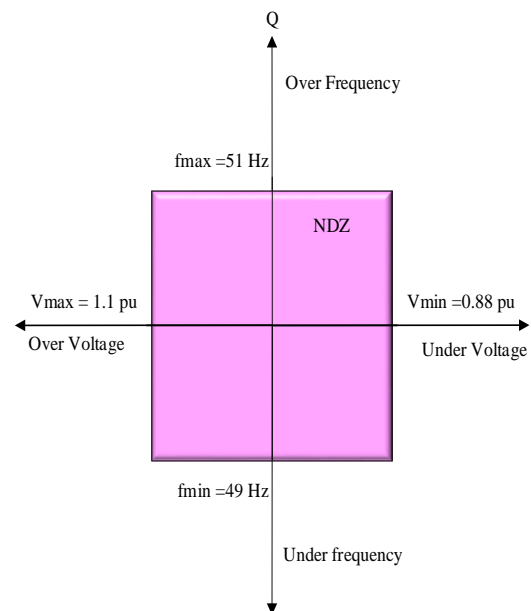


Fig. 5.6: Non Detection Zone of OVP/UV and OFP/UF method

5.5 Voltage Harmonic Injection

When the magnitude and frequency of the PCC voltage was within the threshold range, i.e. in the case of NDZ islanding detection using passive anti-islanding method was very difficult. In that situation more effective method was the implementation of active anti-islanding method. The proposed active anti-islanding method was Voltage Harmonic Injection method. Here a 6th harmonic voltage was injected into the reference signal which was used for the generation of inverter switching signals. The Fig. 5.7 shows the voltage harmonic injection to the reference signal V_{R ref}, V_{Y ref} and V_{B ref}. The voltages V_{R ref}, V_{Y ref} and V_{B ref} represents the PWM modulator reference voltage signals and V_{Rh}, V_{Yh}, and V_{Bh} represents the injected 6th harmonic voltages. Only a 10 % of this harmonic voltage was injected to the system in order to reduce the effect of harmonics in the power quality of the system.

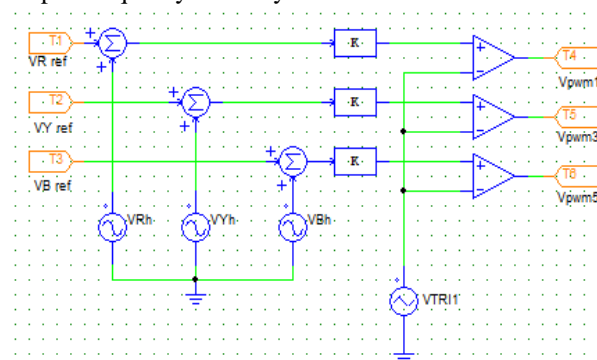


Fig. 5.7: Simulation diagram showing Voltage Harmonic Injection to the system

VI. RESULTS AND DISCUSSIONS

The various simulation results that have been obtained using the software package POWERSIM are shown below. The simulation diagram of the grid connected solar photovoltaic power plant and its controller board are shown in Fig. 5.1 (a) and (b). The current and voltage waveforms of Grid connected solar photovoltaic power plant without and with islanding is shown in Fig. 6.1 and 6.2.

It is clear from the simulation results that, during the grid connected mode the current and voltage are in-phase and if there is any small disturbances during these conditions, since utility grid voltage is stiff, it compensate it and maintain the stability and keep the system in upf. When islanding occurs the equilibrium of the system is disturbed and there will be very high deviations in the PCC voltage magnitude, phase and frequency.

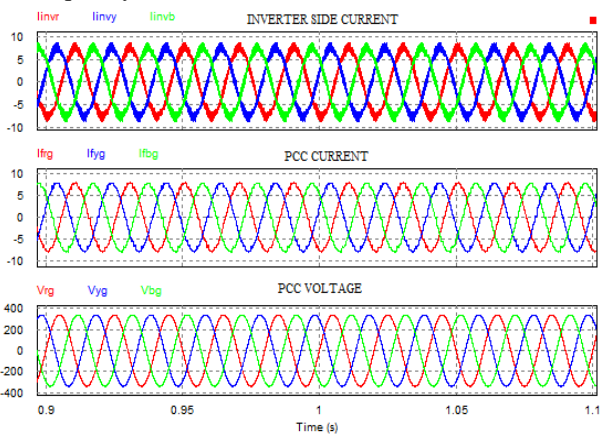


Fig. 6.1: Simulation results without islanding event (a) Inverter side Current (b) PCC Current (c) PCC Voltage

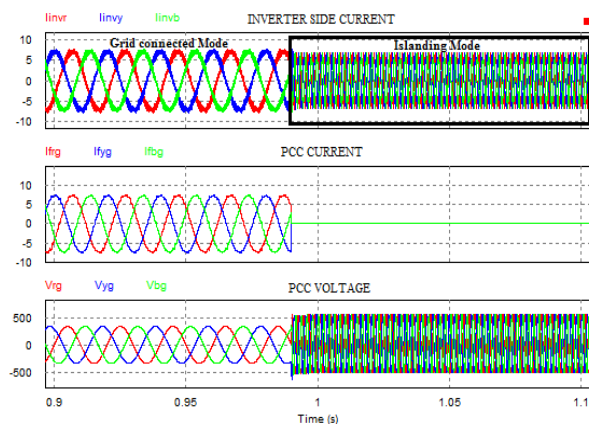
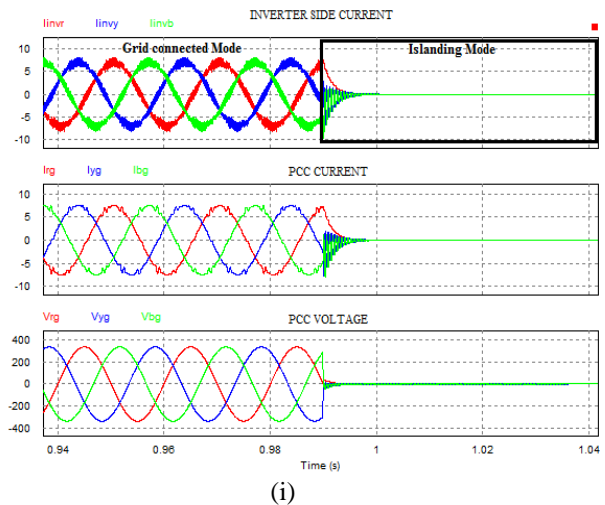


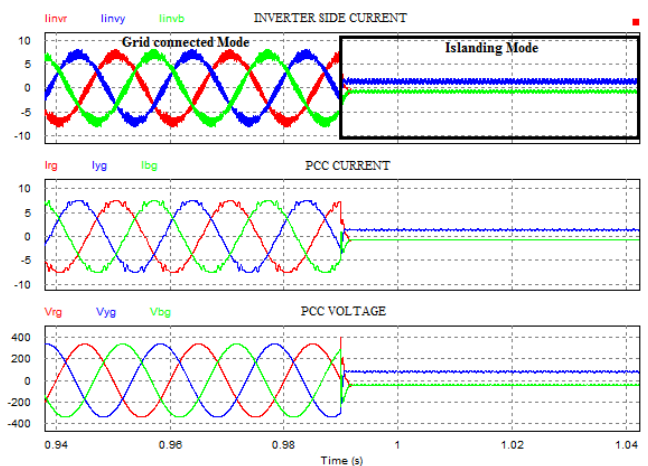
Fig. 6.2: Simulation results with islanding event (a) Inverter side Current (b) PCC Current (c) PCC Voltage during no Load condition

As mentioned earlier, islanding may happen in any section of a grid i.e. in transmission lines, substations, distribution lines, etc. So some valuable

power levels are considered which was shown in the table 5.2, 5.3, and 5.4 and those are simulated using PSIM software. The R, R-L and R-L-C loads are considered for the experimentation. Some of the results are shown in the figure below.

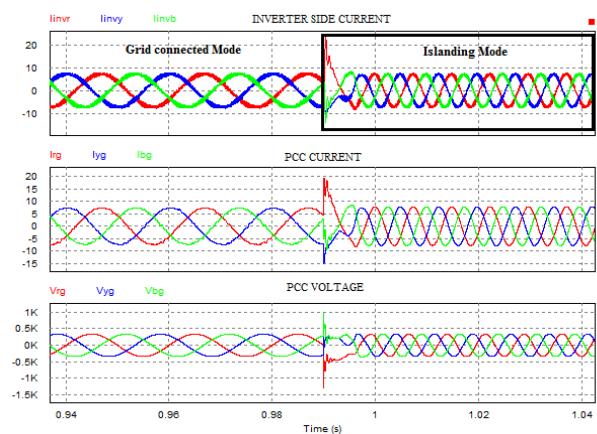


(i)

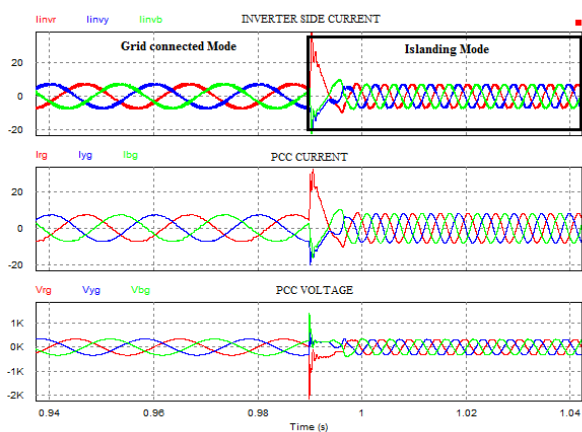


(ii)

Fig. 6.3: Simulation results with islanding event (a) Inverter side Current (b) PCC Current (c) PCC Voltage with R Load; (i) $R = 5.9658\Omega$ (ii) $R = 59.658\Omega$

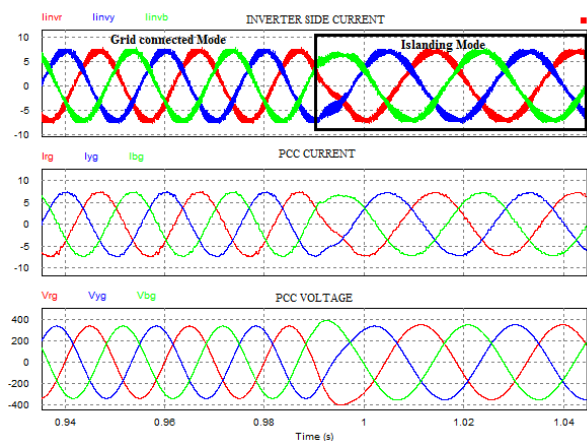


(i)

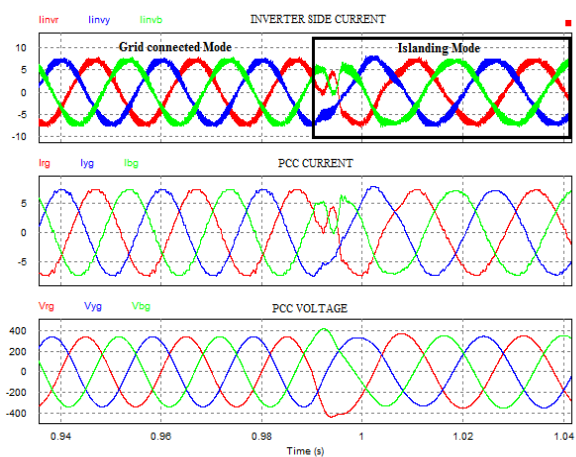


(ii)

Fig. 6.4: Simulation results with islanding event (a) Inverter side Current (b) PCC Current (c) PCC Voltage with R – L Load; (i) R= 59.658Ω, L= 75.959mH (ii) R= 59.658Ω, L= 47.474mH



(i)



(ii)

Fig. 6.5: Simulation results with islanding event (a) Inverter side Current (b) PCC Current (c) PCC Voltage with R - L - C Load; (i) R= 59.658Ω, L= 189.897mH, C= 53.36μF (ii) R= 59.658Ω, L= 75.959mH, C= 133.39μF

From the Fig. 6.5 (ii), it was clear that the magnitude and frequency of the PCC voltage during islanding mode is almost same as that of the grid connected mode and hence islanding detection is difficult. The Fig. 6.5 (ii) shows the waveform of R-L-C load with Q factor 2.5. From the simulation results it was observed that for a Q factor of 2.5 or above for an R-L-C load, the islanding detection was difficult and it indicates a condition of NDZ. The OVP/UVP and OFP/UFM methods were failed. So voltage harmonic injection method was used. The simulation results shown in Fig. 6.6 shows the voltage and current waveforms during grid connected and islanding mode after the injection of 6th harmonic voltage in case of NDZ.

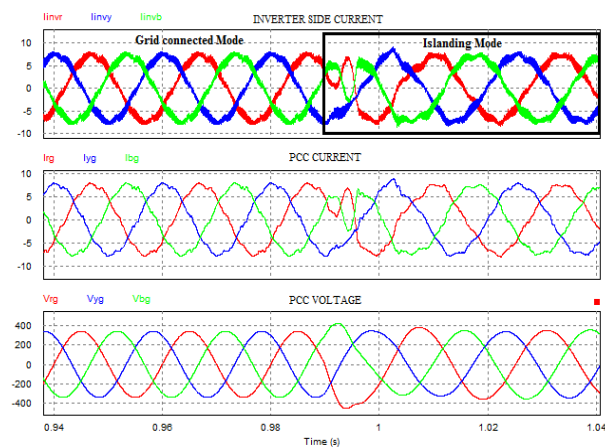


Fig. 6.6: Simulation results with Voltage Harmonic Injection during Non-Detection Zone (a) Inverter side Current (b) PCC Current (c) PCC Voltage with R - L - C Load

After the injection of the 6th harmonic voltage, the THD of the system voltage and inverter current is continuously monitored. From the THD values monitored, the islanding condition was detected. The obtained THD values during NDZ with and without harmonic injection were shown in Fig. 6.7 (i) and (ii).

THD	
Fundamental Frequency	5.0000000e+001 HZ
linvr	3.1373562e-001
linvy	3.6834451e-001
linvb	3.7379926e-001
lrg	3.0625657e-001
lyg	3.6219167e-001
lbg	3.6236552e-001
Vrg	3.4327533e-001
Vry	3.0433915e-001
Vbg	3.7821602e-001
Vstep	3.3791484e+000

(i)

THD	
Fundamental Frequency	5.0000000e+001 HZ
linvr	5.4284329e-001
linvy	3.4655045e-001
linvb	3.5223103e-001
lrg	5.9004405e-001
lyg	3.6303813e-001
lbg	3.5283674e-001
Vrg	4.3409055e-001
Vyg	5.1292728e-001
Vbg	2.8214754e-001
Vstep	2.1630640e+000

(ii)

Fig.6.7: THD values of the waveforms during Islanding mode (a) without voltage harmonic injection (b) with voltage harmonic injection

VII. CONCLUSION

Anti-islanding detection and protection for grid connected PV systems is very important for safety and must exhibit sufficient dependability and security. This paper presents the analysis, modelling and simulation of an active anti-islanding method in three phase grid connected solar photovoltaic power plants. The proposed method, voltage harmonic injection method, injects a 10% of 6th harmonic voltage into the modulating signal in order to detect the islanding event. Modelling and simulation results are given to demonstrate the ability of the proposed method in islanding detection during non-detection zone. The grid connected solar PV model has been implemented using the POWERSIM software package. The behaviour of the proposed scheme was examined under different load operating conditions.

This work aims to find the best solutions that lead to the detection of islanding condition during non-detection zone condition and also for the smart grid applications in which passive method fails. The results confirm that the proposed scheme is a very promising and economical method to satisfy anti-islanding protection requirements for NDZ conditions and for smart grid applications.

REFERENCES

[1] IEEE Standard for Interconnecting Distributed Resources with Electric Power Systems, IEEE Standard 1547-2003, Jul. 2003.
 [2] IEEE Recommended Practice for Utility Interface of Photovoltaic (PV) Systems, IEEE Standard 929-2000, Apr. 2000.
 [3] F. De Mango, M. Liserre, A. D. Aquila, and A. Pigazo, "Overview of antiislanding algorithms for PV systems. Part I: Passive methods," in

Proc.IEEE Power Electron. Motion Control Conf., Aug. 2006, pp. 1878–1883.
 [4] Z. Ye, A. Kolwalkar, Y. Zhang, P. Du, and R. Walling, "Evaluation of antiislanding schemes based on non-detection zone concept," *IEEE Trans.Power Electron.*, vol. 19, no. 5, pp. 1171–1176, Sep. 2004.
 [5] A. Timbus, A. Oudalov, and N. M. Ho Carl, "Islanding detection in smart grids," in *Proc. IEEE Energy Convers. Congr. Expo.*, Sep. 2010, pp. 3631–3637.
 [6] F. De Mango, M. Liserre, and A. D. Aquila, "Overview of anti-islanding algorithms for PV systems. Part II: Active methods," in *Proc. IEEE PowerElectron. Motion Control Conf.*, Aug. 2006, pp. 1884–1889.
 [7] H. Karimi, A. Yazdani, and R. Iravani, "Negative-sequence current injection for fast islanding detection of a distributed resource unit," *IEEE Trans. Power Electron.*, vol. 23, no. 1, pp. 298–307, Jan. 2008.
 [8] A. Yafaoui, B. Wu, and S. Kouro, "Improved active frequency drift antiislanding detection method for grid connected photovoltaic systems," *IEEE Trans. Power Electron.*, vol. 27, no. 5, pp. 2367–2375, May 2012.
 [9] L. A. C. Lopes and H. L. Sun, "Performance assessment of active frequency drifting islanding detection methods," *IEEE Trans. Energy Convers.*, vol. 21, no. 1, pp. 171–180, Mar. 2006.
 [10] H. Vahedi and M. Karrari, "Adaptive fuzzy Sandia frequency-shift method for islanding protection of inverter-based distributed generation," *IEEE Trans. Power Del.*, vol. 28, no. 1, pp. 84–92, Jan. 2013.
 [11] "1547.1 IEEE Standard Conformance Test Procedures for Equipment Interconnecting Distributed resources with Electric Power Systems," *IEEE Std 1547.1-2005*, 2005
 [12] Aleksandr Reznik, Marcelo Godoy Simões, Ahmed Al-Durra, and S. M. Mueyeen, "LCL Filter Design and Performance Analysis for Grid Interconnected Systems," *IEEE Trans. Ind. Appl.*, vol. 50, no. 2, pp. 1225–1232, Mar./Apr. 2014.
 [13] Marco Liserre, Frede Blaabjerg, and Steffan Hansen, "Design and Control of an LCL-Filter-Based Three-Phase Active Rectifier," *IEEE Trans. Ind. Appl.*, vol. 41, no. 5, pp. 1281–1291, Sept./Oct. 2005.
 [14] Xu Renzhong, Xia Lie, Zhang Junjun, and Ding Jie, "Design and Research on the LCL Filter in Three-Phase PV Grid-Connected Inverters," *International Journal of Computer and Electrical Engineering*, Vol. 5, No. 3, pp. 322-325, June 2013.
 [15] IEEE Guide for Design , Operation , and Integration of Distributed Resource Island Systems with Electric Power Systems, IEEE Standard 1547.4, 2011.